

Type-II/type-II band alignment to boost spatial charge separation: A case study of g-C₃N₄ quantum dot/a-TiO₂/r-TiO₂ for highly efficient photocatalytic hydrogen and oxygen evolution

Bing-Xin Zhou,^a Shuang-Shuang Ding,^a Yan Wang,^a Xiao-Rui Wang,^a Wei-Qing Huang,^{*,a} Kai Li,^b Gui-Fang Huang^{*,a}

¹Department of Applied Physics, School of Physics and Electronics, Hunan University, Changsha 410082, China

^bState Key Laboratory of Powder Metallurgy, Central South University, Changsha 410083, China

Experimental section

QCN preparation

The QCN was fabricated by previously reported method.¹ Firstly, The bulk CN was prepared by heating melamine at 500 °C for 2 h, with a heating rate of 5 °C min⁻¹. 1 g bulk CN was treated in the mixture of concentrated H₂SO₄ (20 mL) and HNO₃ (20 mL) for about 2 h at room temperature. The mixture was then diluted and washed for several times with deionized water, the as-obtained white product was porous CN (Fig. S1). Then, 200 mg of the porous CN was dispersed in 60 mL concentrated NH₃·H₂O, and the suspension was transferred to a poly(tetrafluoroethylene) (Teflon)-lined autoclave (100 mL) and heated at 180 °C for 12 h. After cooling to room temperature, the obtained solution was ultrasound for about 6 h and centrifuged at 5000 rpm for 10 minutes. The bottom precipitate was removed. The final obtained concentration of QCN was about 1.2 mg/mL (PH=14).

QCN/a-TiO₂/r-TiO₂/ preparation

The T-II/T-II heterojunctions of QCN/a-TiO₂/r-TiO₂ were synthesized via a simple mixing method followed by heat treatment. The commercially available titanium dioxide, Degussa P25 (containing 70% a-TiO₂ and 30% r-TiO₂) was used here. In a typical preparation procedure, 200 mg P25 was dispersed in 50 mL distilled water and sonicated for 30 min. Subsequently, a certain amount

*. Corresponding author. *E-mail address*: wqhuang@hnu.edu.cn
E-mail address: gfhuang@hnu.edu.cn

of QCN solution was added and stirred at 110 °C for 3 h by oil bath reflux. Then the mixed solution of P25 and QCN is heated until the aqueous solution was completely evaporated and dried at 60 °C overnight. Finally, the residual mixture powder was placed in a crucible and heated in a muffle furnace at 500 °C for 1 h to obtain the final T-II/T-II heterojunctions of QCN/a-TiO₂/r-TiO₂. When the volume of the QCN solution was 5, 10, and 15 mL, the obtained samples were labeled as P25-QCN1, P25-QCN2, and P25-QCN3, respectively. The hydroxylated P25 can be obtained by adding 2 mL ammonium hydroxide instead of QCN solution in the same process. Subsequently the hydroxylated P25 was washed several times with deionized water by centrifugation until the pH of the solution was neutral and then dried at 60 °C overnight.

Characterization

The morphological details of prepared samples were probed by an S-4800 field emission scanning electron microscopy (SEM) operating at an accelerating voltage of 5 kV. The crystallographic structure of the samples was characterized by power X-ray diffraction (XRD, Siemens D-5000) and high-resolution field emission transmission electron microscopy (HRTEM, FEI Tecai-F20). The UV-vis absorption spectras was obtained from a Shimadzu UV3600 spectrophotometer equipped with a 60 mm diameter integrating sphere using BaSO₄ as reference. The chemical compositions were measured through X-ray photoelectron spectroscopy (XPS, PHI Quantera x-ray photoelectron spectrometer with 300W Al K α radiation). Photoluminescence (PL) spectra were recorded using fluorescence spectrophotometer on an F-2500 fluorescence spectrometer with xenon lamps. The excitation wavelength of the P25-QCN heterojunction is 100 nm. The excitation wavelength of bulk CN and QCN is 350 nm.

Photocatalytic degradation of MB

The photocatalytic behavior for the degradation of 10 mg/L methylene blue (MB, 80 mL) with 20 mg samples under visible light irradiation. A low-power 55 W compact fluorescent lamp was chosen as the visible light. Prior to irradiation, the solution suspend with photocatalysts were sonicated in the dark for 30 min to reach the adsorption-desorption equilibrium. 4 mL reaction solutions were with draw at regular time intervals and centrifuged to remove the catalyst sample before being analyzed by UV-vis absorption spectroscopy (UV-2450, Shimadzu). The degradation efficiency can be evaluated by the function $C_t/C_0 \times 100\%$, where C_0 was the initial concentration

of MB and C_t was the concentration after degradation.

Photocatalytic hydrogen and oxygen production

The photocatalytic water splitting to H_2 and O_2 was carried out in a Pyrex glass reaction cell connected to a glass-closed system, and a magnetic control pump was used to make sure the gas in the reaction system cycles well.

For the hydrogen production, 50 mg prepared samples powders were dispersed in 333 mL aqueous solution containing methanol (10 vol%). Co-catalyst (1 wt% Pt) was introduced by in-situ photodeposition from the precursor of $H_2PtCl_6 \cdot 6H_2O$. The system was vacuum-treated several times to remove the dissolved air. The reaction was conducted under a 300W Xeon-lamp (Simulated sunlight) or 300 W halogen lamp (Visible light). Meanwhile, the cooling water was used to maintain the temperature at 10 °C. The evolved gas was analyzed by gas chromatography equipped with a thermal conductive detector (TCD) and a 5 Å molecular sieve column, using argon gas as the carrier gas.

For the oxygen production, 50 mg of photocatalysts were well dispersed in an aqueous solution (100 mL) containing $AgNO_3$ (0.01 M) as an electron acceptor and La_2O_3 (200 mg) as a pH buffer agent. The $Co(OH)_2$ cocatalyst was loaded by an immersion method reported previously.² In a typical synthesis, 50 mg of samples was immersed into 80 mL aqueous solutions containing 4.7 mg of $Co(NO_3)_2 \cdot 6H_2O$. Subsequently, the mixture was sonicated for 30 min to achieve a homogenous suspension. Then 0.5 mL $NH_3 \cdot H_2O$ was added dropwise into the above solution. The final hybrid photocatalyst was obtained after washing with water and drying in a vacuum oven at 80 °C for 10 h. The other test conditions were consistent with hydrogen production.

Photoelectrochemical measurements

The electrochemical and photoelectric properties were performed on a CHI660E electrochemical system (Shanghai, China) using a standard three-electrode cell with a working electrode, a platinum wire counter electrode, and an Ag/AgCl reference electrode. The Na_2SO_4 (0.1 M) was used as the electrolyte solution. All the electrochemical measurements were performed under room temperature. To prepare the working electrode, 1 mg catalyst with 0.5 mL ethanol and 25 μ L Nafion solution (5 vol%) were mixed ultrasonically for 30 min. Then, the suspension was dip-coating onto the F-doped tin oxide (FTO) glass electrode ($1 \times 1 \text{ cm}^2$) with heating at 80 °C.

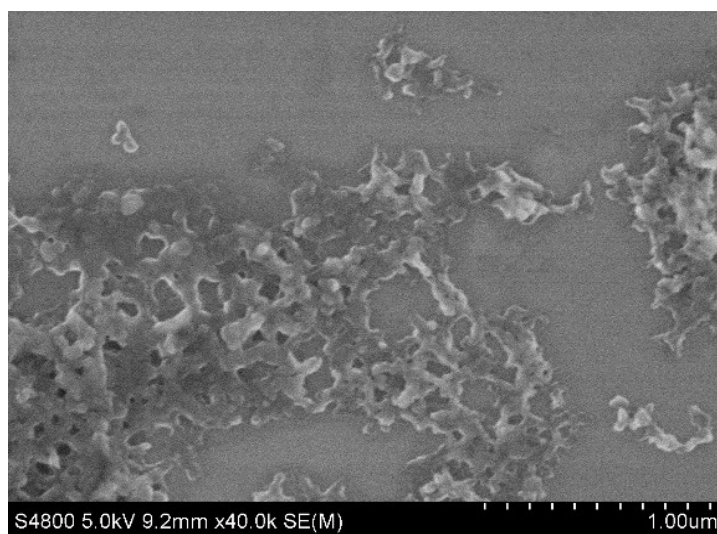


Fig. S1 The SEM of $g\text{-C}_3\text{N}_4$ nanosheets.

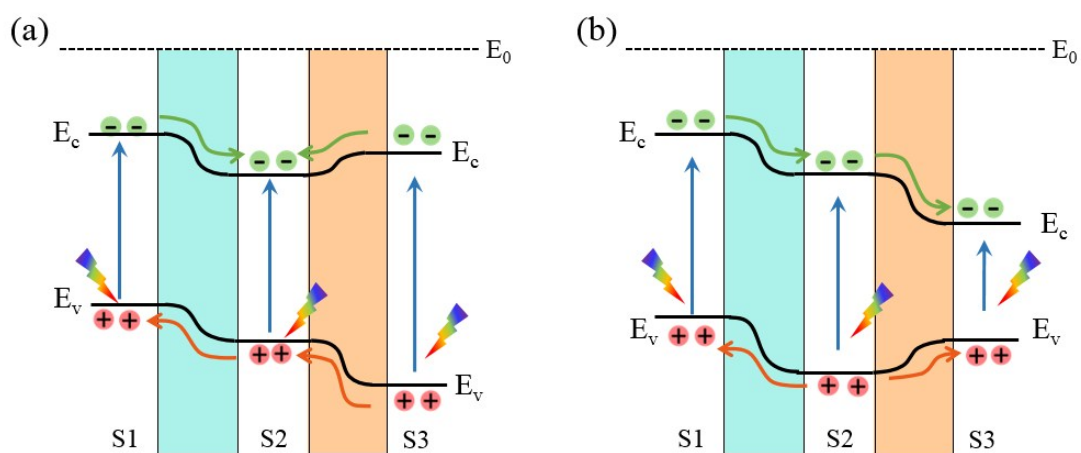


Fig. S2 Schematic illustrating the band gap alignment and charge flow of a T-II/TI double heterojunction.

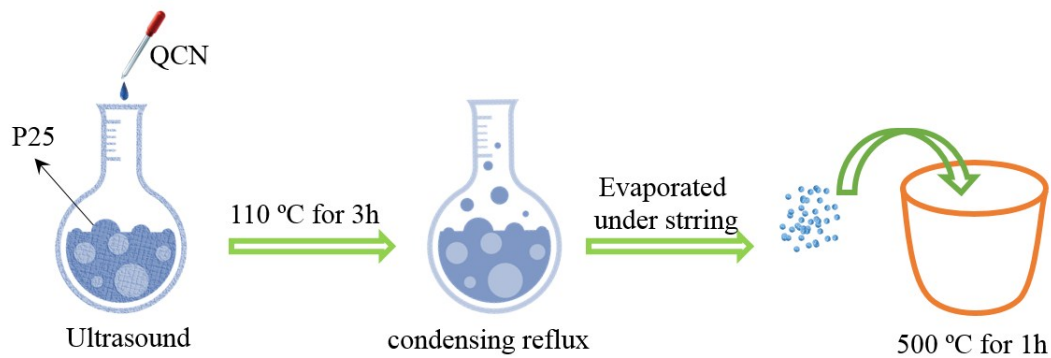


Fig. S3 The preparation process of P25-QCN composites.

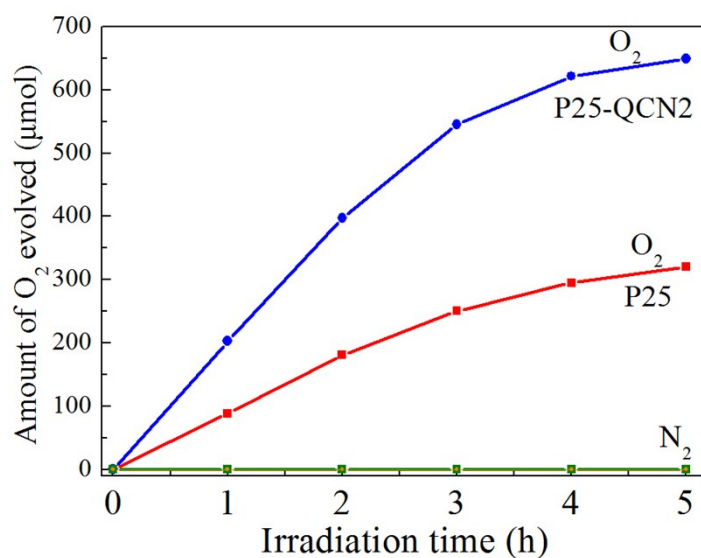


Fig. S4 Amount of O₂ produced of P25 and P25-QCN2 under simulated sunlight irradiation.

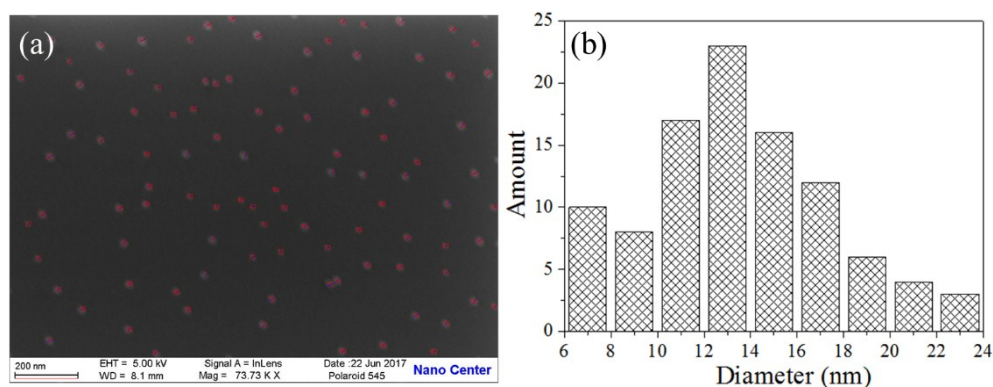


Fig. S5 The (a) SEM image and (b) particle size statistical distribution of QCN.

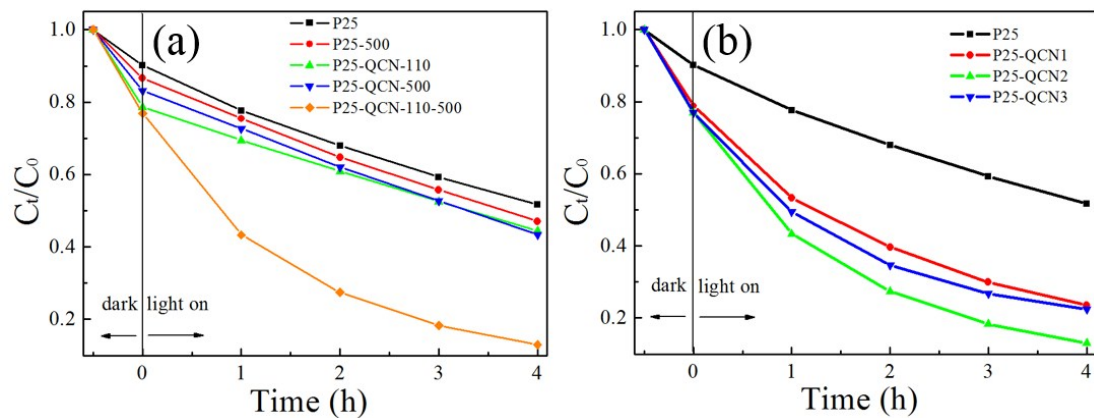


Fig. S6 (a) The effect of preparation methods on photocatalytic degradation of MB in P25-QCN composites. (b) Photocatalytic activities of samples (20 mg) for degradation of MB (10 mg/L, 80 mL) under visible light irradiation.

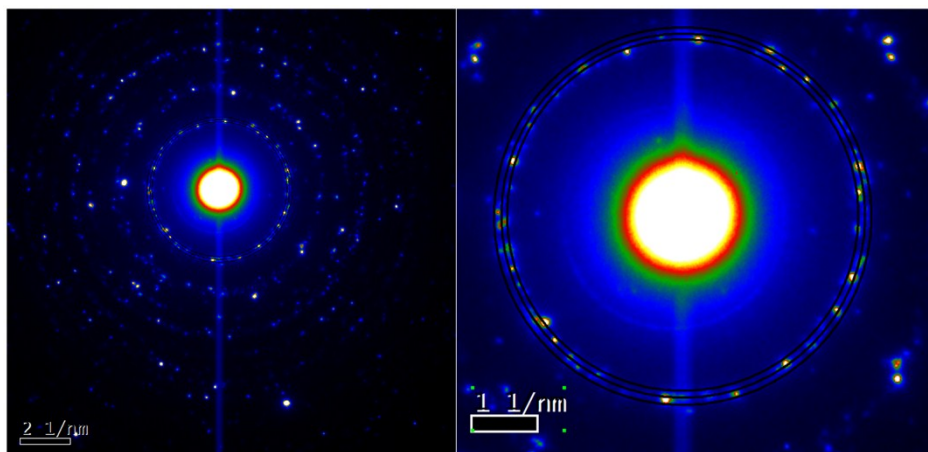


Fig. S7 The SAED images of P25-QCN2.

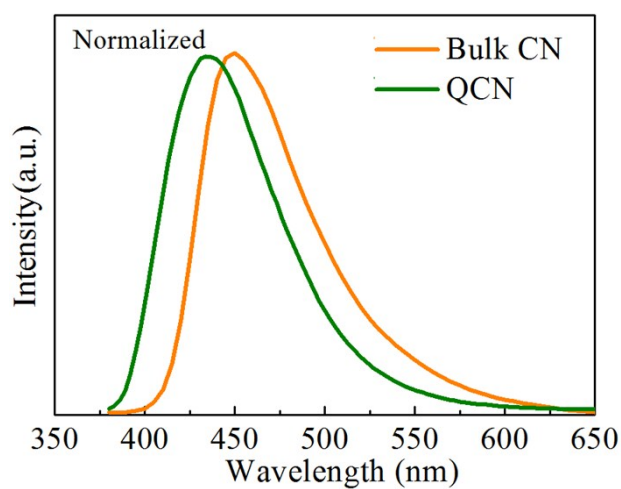


Fig. S8 The normalized PL spectra of bulk CN and QCN.

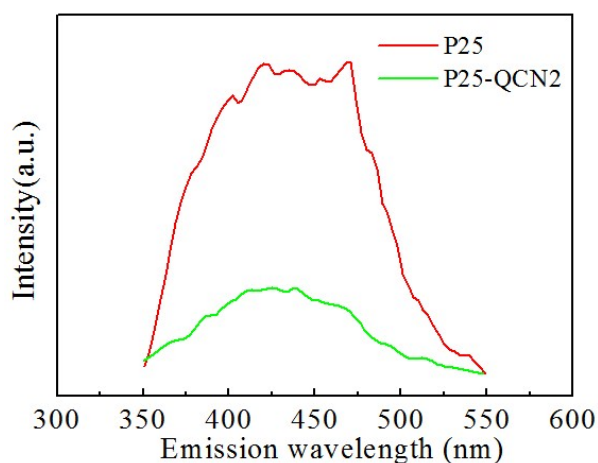


Fig. S9 PL spectra of P25 and P25-QCN2 at excitation wavelength of 300 nm.

Table S1 Comparison of studies concerning $\text{TiO}_2/\text{g-C}_3\text{N}_4$ heterojunctions for photocatalytic water splitting

Dimensi onality	Samples	co-catalyst	sacrificial agent	light source	HER $\mu\text{mol/h}\cdot\text{g}$	Ref
2D/2D	<i>Anatase</i> $\text{TiO}_2/\text{O-g-}$ C_3N_4	3 wt% Pt	20 vol% TEOA	300W Xe $\lambda > 400 \text{ nm}$	587.1	3
2D/2D	<i>Anatase</i> $\text{TiO}_2/\text{g-C}_3\text{N}_4$	-	10 vol% ethanol	300W Xe $\lambda > 420 \text{ nm}$	350	4
2D/2D	<i>Anatase</i> $\text{TiO}_2/\text{g-C}_3\text{N}_4$	3 wt% Pt	20 vol% TEOA	300W Xe $\lambda > 400 \text{ nm}$	587	5
2D/2D	<i>Anatase</i> $\text{TiO}_2/\text{g-C}_3\text{N}_4$	$\sim 0.3 \text{ wt\% Pt}$	20 vol% methanol	300W Xe $\lambda > 400 \text{ nm}$	1960	6
0D/2D	<i>Anatase</i> $\text{TiO}_2/\text{g-C}_3\text{N}_4$	3 wt% Pt	10 vol% TEOA	250W visible light source	1041.6	7
3D	<i>Anatase</i> $\text{TiO}_2/\text{g-C}_3\text{N}_4$	1 wt% Pt	10 vol% TEOA	300W Xe	726.0	8
core- shell	<i>Anatase</i> $\text{TiO}_2/\text{g-C}_3\text{N}_4$	1 wt% Pt	10 vol% methanol	500W Xe	625.5	9

core-shell	<i>Anatase</i> <i>B-TiO₂/g-C₃N₄</i>	-	10 vol% TEOA	300W Xe lamp	808.97	10
	<i>Anatase</i> <i>/brookite</i> <i>TiO₂/g-C₃N₄</i>	1 wt% Pt	10 vol% TEOA	800W Xe- Hg $\lambda > 420$ nm	30.0	11
	<i>P25/g-C₃N₄</i>	1 wt% Pt	10 vol% TEOA	800W Xe $\lambda > 420$ nm	5.4	11
	<i>Brookite</i> <i>TiO₂/g-C₃N₄</i>	1 wt% Pt	10 vol% TEOA	300W Xe $\lambda > 400$ nm	1058	12
	<i>C-TiO₂/g-C₃N₄</i>	3 wt% Pt	10 vol% TEOA	300W Xe $\lambda < 420$ nm	1145.6	13
	<i>P25/g-C₃N₄</i>	1 wt% Pt	10 vol% TEOA	300W Xe $\lambda > 420$ nm	1780.0	13
	<i>C,N-TiO₂/g-C₃N₄</i>	No	10 vol% TEOA	300W Xe $\lambda > 400$ nm	39.2	14
	<i>anatase</i> <i>TiO₂/g-C₃N₄</i>	3 wt% Pt	10 vol% TEOA	300W Xe $\lambda > 420$ nm	800	15
0D/0D	<i>P25-QCN2</i>	1 wt% Pt	10 vol% methanol	300W Xe	30528 (1526.4 $\mu\text{mol/h}$)	This work
0D/0D	<i>P25-QCN2</i>	1 wt% Pt	10 vol% methanol	300W Hg $\lambda > 400$ nm	986 (49.3 $\mu\text{mol/h}$)	This work
0D/0D	<i>P25-QCN2</i>	1 wt% Pt	10 vol% TEOA	300W Hg $\lambda > 400$ nm	8748 (437.4 $\mu\text{mol/h}$)	This work

References

- 1 X. Zhang, H. Wang, H. Wang, Q. Zhang, J. Xie, Y. Tian, J. Wang and Y. Xie, *Adv. Mater.*, 2014, **26**, 4438-4443.
- 2 D. Zhao, C. L. Dong, B. Wang, C. Chen, Y. C. Huang, Z. Diao, S. Li, L. Guo and S. Shen, *Adv. Mater.*, 2019, 31, 1903545.
- 3 R. Zhong, Z. Zhang, H. Yi, L. Zeng, C. Tang, L. Huang and M. Gu, *Appl. Catal., B*, 2018, **237**, 1130-1138.
- 4 Y. Yang, X. Li, C. Lu and W. Huang, *Catal. Lett.*, 2019, **149**, 2930-2939.

- 5 R. Zhong, Z. Zhang, S. Luo, Z. C. Zhang, L. Huang and M. Gu, *Catal. Sci. Technol.*, 2019, **9**, 75-85.
- 6 W.-S. Liu, L.-C. Wang, T.-K. Chin, Y.-C. Yen and T.-P. Perng, *RSC Adv.*, 2018, **8**, 30642-30651.
- 7 M. A. Alcudia-Ramos, M. O. Fuentes-Torres, F. Ortiz-Chi, C. G. Espinosa-Gonzalez, N. Hernandez-Como, D. S. Garcia-Zaleta, M. K. Kesarla, J. G. Torres-Torres, V. Collins-Martinez and S. Godavarthi, *Ceram. Int.*, 2020, **46**, 38-45.
- 8 M. Wu, J. Zhang, C. Liu, Y. Gong, R. Wang, B. He and H. Wang, *ChemCatChem*, 2018, **10**, 3069-3077.
- 9 M. A. Mohamed, M. F. M. Zain, L. J. Minggu, M. B. Kassim, J. Jaafar, N. A. S. Amin and Y. H. Ng, *Appl. Surf. Sci.*, 2019, **476**, 205-220.
- 10 J. Pan, Z. Dong, B. Wang, Z. Jiang, C. Zhao, J. Wang, C. Song, Y. Zheng and C. Li, *Appl. Catal., B*, 2019, **242**, 92-99.
- 11 Q. Tay, X. Wang, X. Zhao, J. Hong, Q. Zhang, R. Xu and Z. Chen, *J. Catal.*, 2016, **342**, 55-62.
- 12 Y. Zang, L. Li, Y. Xu, Y. Zuo and G. Li, *J. Mater. Chem. A*, 2014, **2**, 15774-15780.
- 13 C. Yang, J. Qin, Z. Xue, M. Ma, X. Zhang and R. Liu, *Nano Energy*, 2017, **41**, 1-9.
- 14 W. Chen, T.-Y. Liu, T. Huang, X.-H. Liu, G.-R. Duan, X.-J. Yang and S.-M. Chen, *RSC Adv.*, 2015, **5**, 101214-101220.
- 15 H. Zhang, F. Liu, H. Wu, X. Cao, J. Sun and W. Lei, *RSC Adv.*, 2017, **7**, 40327-40333.